Performance Improvement of the Wald Test for GPS RTK with the Assistance of INS

Mamoun F. Abdel-Hafez, Dae Je Kim, Eunsung Lee, Sebum Chun, Young Jae Lee*, Taesam Kang, and Sangkyung Sung

Abstract: To use the Global Positioning System (GPS) carrier phase measurement for precise positioning, the integer ambiguities at the early stage of most algorithms must be determined. Furthermore, if a precise positioning is to be applied to real time navigation, fast determination and validation methods for integer ambiguity are essential. In this paper, the Wald test that simultaneously determines and validates integer ambiguities is used with assistance of the Inertial Navigation System (INS) to improve its performance. As the Wald test proceeds, it assigns a higher probability to the candidate that is considered to be true at each time step. The INS information is added during the Wald test process. Large performance improvements were achieved in convergence time as well as in requiring fewer observable GPS satellites. To test the performance improvement of the Wald test with the INS information, experimental tests were conducted using a ground vehicle. The vehicle moved in a prescribed trajectory and observed seven GPS satellites. To verify the effect of the INS information on the Wald test, the convergence times were compared with cases that considered the INS information and cases that did not consider the INS information. The results show that the benefits of using the INS were emphasized as fewer GPS satellites were observable. The performance improvement obtained by the proposed algorithm was shown through the fast convergence to the true hypothesis when using the INS measurements.

Keywords: Fault detection, GPS, INS, integer ambiguity, real-time kinematic.

1. INTRODUCTION

A wide range of GPS applications require achieving centimeter-level accuracy. For those applications, GPS carrier phase measurements are very promising tools. Therefore, significant contributions have been made to obtain fast, reliable methods to fix carrier phase integer ambiguity. Once this integer ambiguity is resolved, the carrier phase measurements can be used as high accuracy range measurements.

Manuscript received February 25, 2007; revised November 22, 2007; accepted March 20, 2008. Recommended by Editorial Board member Hyo-Choong Bang under the direction of Editor Jae Weon Choi. This research was supported by a grant from Air Transportation Advancement Program (ATAP) funded by Ministry of Land, Transportation and Maritime Affairs (MLTM) of Korean government.

Mamoun F. Abdel-Hafez is with American University of Sharjah, Sharjah, United Arab Emirates (e-mail: mabdelhafez @aus.edu).

Dae Je Kim is with R&D center at the Hyundai Rotem, Korea (e-mail: kd76@nate.com).

Eunsung Lee is with Korea Aerospace Research Institute, Korea (e-maill: koreagnss@kari.re.kr).

Sebum Chun is with Microinfinity Co.,Ltd, Korea (e-mail: sbchun@minfinity.com).

Young Jae Lee, Taesam Kang and Sangkyung Sung are with Department of Aerospace Engineering, Konkuk University, Korea (e-mails: {younglee, tskang, sksung}@konkuk.ac.kr).

* Corresponding author.

During the last decade, many integer ambiguity resolving methods have been proposed, and Teunissen's least-squares ambiguity decorrelation adjustment (LAMBDA) method has been the most popular. This method is known to be efficient in processing data using a very efficient transformation [1] and must be followed by an integer ambiguity validation process after the integer ambiguity is estimated as in most integer ambiguity fixing methods. However, the multiple hypotheses Wald sequential probability ratio test (MHWSPRT) is a method that validates integer ambiguity during the initial ambiguity resolution [2]. For convenience, hereafter the Wald test refers to MHWSPRT. The Wald test has been found to be a very efficient method to converge to the correct integers. This method is essentially a nonlinear sequential filter which, after conditioning the measurements, is optimal [3].

It is well known that the characteristics of GPS and INS are very much distinguishable: the strong point of one system is the weak point of the other [4]. INS has characteristics of error accumulation, anti-interference, self-operability, short time stability, and a high data rates. For this reason, during the last two decades, there have been many attempts to use and obtain synergistic effects between GPS and INS. Velocity and position information from GPS are used to obtain

ideal performance from INS [5]. Traditionally, an integrated INS/GPS has been executed in a loosely or tightly coupled method through the Kalman filter [6]. For example, the GPS/INS alignment errors can be made observable by maneuvering a vehicle based on the observability analysis of the time-varying system [7]. The loosely coupled method and the combination of the fast ambiguity search filter (FASF) and LAMBDA methods have been used for ambiguity resolution in real time kinematic (RTK) satellite navigation [8]. As a possible alternative, a cheaper and poorer quality INS may be investigated. A combination of the FASF methods has been used for ambiguity resolution in the RTK navigation system. Furthermore, a neural network has been applied for multi-sensor integration, which suggests a multi-sensor integration approach to fuse data from an INS and a DGPS using multi-layer feed-forward neural networks with a back propagation learning algorithm [9].

The GPS integer ambiguity fixing problem consists of two distinct parts: the ambiguity *estimation* problem and the ambiguity *validation* problem [1]. The first part determines the optimal estimation for unknown variables using observation equation models. The second part validates the estimated ambiguities and determines whether the estimated integer ambiguity solution from the first part is accepted or not. In most cases, the second part is independent of the estimation and is extremely important for safety sensitive applications.

However, the Wald test is a method that estimates the initial ambiguity and simultaneously validates the integer ambiguity [2]. In [2] and [3], it has been shown that the Wald test is a well-proven and efficient integer ambiguity resolution algorithm and that the biggest advantage of the Wald sequential test is that it has one simple unified step for the estimation and validation of the integer ambiguities of GPS carrier phase measurements.

The objective of this paper is to improve the performance of the Wald test in resolving the integer ambiguity of GPS carrier phase measurements with the assistance of INS measurements. The proposed algorithm consists of three parts: the initial positioning using GPS code information, integrating the GPS and INS information, and determining the integer ambiguity using the Wald test. As a result, we can observe the direct contribution of the INS information to the Wald test in a short convergence time and in a functional capability of fewer observable satellites.

In Section 2, a brief review of the Wald test is presented. In Section 3, the proposed GPS and INS integration is explained in detail. To prove the effectiveness of the developed algorithm, experiments were conducted and the results are analyzed in Section 4. Finally, the conclusions are summarized in Section 5.

2. THE WALD TEST

The Wald test is a special case of the multiple hypothesis Shiryayev sequential probability ratio test: it determines the most likely event from a set of hypotheses assuming that the event is true for all time. The Wald test can be used to obtain the conditional probability that each integer ambiguity under consideration is true. Hence, the Wald test is a statistical method used to validate integer ambiguity. The method forms residuals that are used to obtain the probability of a certain integer hypothesis being the correct integer ambiguity [2]. For more details, refer to [2] and [3].

$F_i(k)$, which is the possibility of the ith integer ambiguity N_i being true given $R(k)$, is defined as:

$$F_i(k) = p(N_i \,|\, R(k)), \tag{1}$$

where the $R(k)$ is the measurement residual history until time k, and i ($i=1...m$) is the index of the hypotheses. $F_i(k)$ is the probability that the ith integer ambiguity is true given the set of residual $R(k)$. Using (1) and Bayes' rule, (2) is derived as follows:

$$F_i(k) = \frac{P\left(N_i, r(k) \,|\, R(k-1)\right)}{P\left(r(k) \,|\, R(k-1)\right)}, \tag{2}$$

where $r(k)$ is the measurement residual vector at time k. The numerator of (2) can be expressed as in (3):

$$\begin{aligned} &P\left(N_i, r(k) \,|\, R(k-1)\right) \\ &\quad = P\left(r(k) \,|\, N_i, R(k-1)\right) \cdot P\left(N_i \,|\, R(k-1)\right), \end{aligned} \tag{3}$$

where $r(k)$ is independent and has the same distribution (iid). Hence, the right side of (3) is described as:

$$P\left(r(k) \,|\, N_i, R(k-1)\right) = P\left(r(k) \,|\, N_i\right) \equiv f_i\left(r(k)\right), \tag{4}$$

$$P\left(N_i \,|\, R(k-1)\right) \equiv F_i(k-1). \tag{5}$$

Substituting (3) into (4), (5) becomes:

$$P\left(N_i, r(k) \,|\, R(k-1)\right) = f_i\left(r(k)\right) \cdot F_i(k-1), \tag{6}$$

The denominator of (2) is described as:

$$\begin{aligned} P\left(r(k) \,|\, R(k-1)\right) &= P_i\left(r(k)\right) \\ &= \sum_{j=1}^{m} P\left(N_j, r(k) \,|\, R(k-1)\right) \\ &= \sum_{j=1}^{m} f_j\left(r(k)\right) \cdot F_j(k-1). \end{aligned} \tag{7}$$

Substituting (2) into (6), (7) is derived as follows:

$$F_i(k) = \frac{F_i(k-1)\cdot f_i\left(r(k)\right)}{\sum_{j=1}^{m} F_j(k-1)\cdot f_j\left(r(k)\right)}, \tag{8}$$

where $f_i(r(k))$ is the probability density function of a residual vector calculated by the ith candidate of the integer ambiguity. By the Gaussian distribution assumption of $r(k)$, $f_i(r(k))$ is described as:

$$f_i\left(r(k)\right) = C\cdot\exp\left\{-\frac{1}{2}r_i(k)^T W_r r_i(k)\right\}, \tag{9}$$

where C is a factor, $Q_r = \begin{bmatrix} Q_{carrier} & 0 \\ 0 & Q_{GPS/INS} \end{bmatrix}$, and $W_r = Q_r^{-1}$.

Using (8), the Wald test computes the probability that a candidate integer is a true integer. After starting with an initial condition that all the candidates have the same probability, the Wald test assigns a higher probability to the highly-seeming-to-be-true integer as it processes the measurement residuals and a lower probability to other integers. From the definition of probability, it is always true that summing all probabilities assigned to all candidates results in one [10]. The Wald test declares one true integer when its probability reaches a predefined threshold very close to one, for example 0.999. In this case, the other integers are very close to zero. For the real-time use of GPS carrier phase measurements for precise position areas, the time taken to reach the threshold is very important for performance as an integer ambiguity resolution algorithm.

3. GPS/INS INTEGRATED SYSTEM

The proposed GPS/INS integrated algorithm is divided into three modules as shown in Fig. 1. The first module computes the initial position of the mobile user using GPS code measurements. The second module has a Kalman filter which computes the mobile position and INS errors using the results of the first module and the inertial measurements of the INS. The last module combines the results from Module 2 and the GPS carrier measurements. This generates the estimated GPS measurements from the results of the second module and finally fixes the integer ambiguity using the Wald test.

The first module of the proposed algorithm computes the initial position of the mobile user using a conventional DGPS process. The resulting initial position is used as the initial position of the INS and the initial condition of the integrated GPS/INS filter. Hereafter, "A" denotes the known reference point and

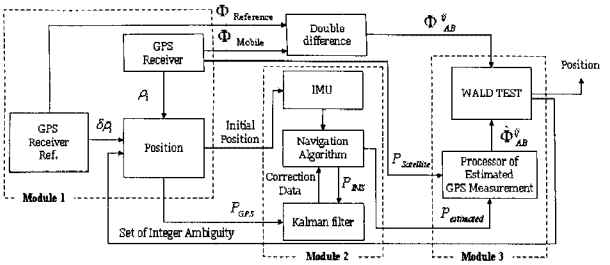

Fig. 1. Block diagram of an integrated system.

"B" denotes the unknown mobile position. Using the GPS code measurements, Module 1 computes the mobile position. The measurements equation is as follows:

$$\rho_B^i = \sqrt{(x^i-\hat{x}_B)^2+(y^i-\hat{y}_B)^2+(z^i-\hat{z}_B)^2}+v_B^i, \tag{10}$$

where ρ_B^i is the distance between the mobile unit and the satellites using code measurements, x^i, y^i, z^i are the coordinates of the ith satellite, $\hat{x}_B$, $\hat{y}_B$, $\hat{z}_B$ are the estimated coordinates of the mobile using code measurements, and v_B^i is the GPS code measurement noise.

Two key processes are performed in Module 2 as seen in Fig. 2. The first key process estimates the position and velocity of the mobile user using IMU measurements. The second estimates the errors of the state variables using the Kalman filter, and these errors are fed back into the first process to compensate the resulting position and velocity. The measurements of the Kalman filter are the difference between the position and the velocity from the GPS and INS. The state variables of the filter are position, velocity, altitude, and inertia sensor biases. The initial alignment is conducted statically at the beginning of the process and is designed to start before the inertial navigation begins. Equation (11) is the system equation of the Kalman filter. The state variables are position error, velocity error, altitude error, and inertia sensor biases with respect to the north, east, and down directions.

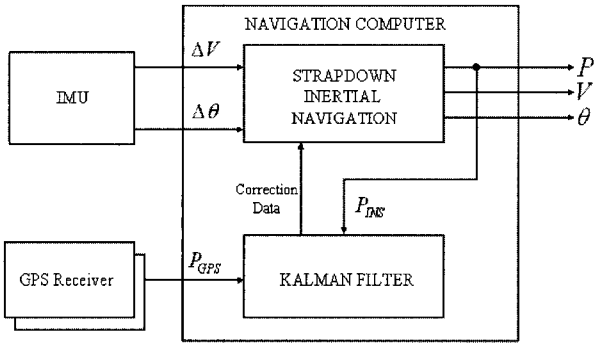

Fig. 2. Structure of the Kalman filter in module 2.

$$\begin{bmatrix} \dot{\mathbf{x}}_{nav} \\ \dot{\mathbf{x}}_{sensor} \end{bmatrix} = \begin{bmatrix} F_{11} & F_{12} \\ 0_{6\times 9} & 0_{6\times 6} \end{bmatrix} \begin{bmatrix} \mathbf{x}_{nav} \\ \mathbf{x}_{sensor} \end{bmatrix} + \begin{bmatrix} w_{nav} \\ 0 \end{bmatrix},$$
$$w_{nav} \sim N(0, Q),$$
$$\mathbf{x}_{nav} \equiv [\delta p_N \ \delta p_E \ \delta p_D \ \delta v_N \ \delta v_E \ \delta v_D \ \delta\psi_N \ \delta\psi_E \ \delta\psi_D]^T, \quad (11)$$
$$\mathbf{x}_{sensor} \equiv [\delta f_x \ \delta f_y \ \delta f_z \ \delta\varepsilon_x \ \delta\varepsilon_y \ \delta\varepsilon_z]^T,$$

where Q is a covariance matrix of the process noise, δp_N, δp_E, δp_D are the position errors in the NED coordinates, δv_N, δv_E, δv_D are the velocity errors in the NED coordinates, $\delta\psi_N$, $\delta\psi_E$, $\delta\psi_D$ are the altitude errors in the NED coordinates, δf_N, δf_E, δf_D are the accelerometer biases in the body coordinates, and $\delta\varepsilon_N$, $\delta\varepsilon_E$, $\delta\varepsilon_D$ are the gyro biases in the body coordinates.

C_b^n is the direction cosine matrix from the body to the navigation coordinates, R_e is the radius of the Earth, v_N, v_E, v_D are the velocity of north, east and down directions, Ω is the earth rotation rate, L is longitude, h is height, g_n is the Earth's gravity, and f_N, f_E, f_D are specific forces [11].

Equation (12) is the measurement equation of the filer, which uses the differenced position solutions from the GPS and INS.

$$\mathbf{z} = \mathbf{H}\mathbf{x} + \mathbf{v}, \quad \mathbf{v} \sim N(0, R),$$
$$\mathbf{x} = \begin{bmatrix} \mathbf{x}_{nav} \\ \mathbf{x}_{sensor} \end{bmatrix}, \quad \mathbf{z} \equiv \begin{bmatrix} \delta r_N & \delta r_E & \delta r_D \end{bmatrix}^T, \quad (12)$$
$$H = \begin{bmatrix} I_{3\times 3} & 0_{3\times 12} \end{bmatrix},$$

where $\delta r_N, \delta r_E, \delta r_D$ are the differenced position solutions from the GPS and INS in the NED coordinates and R is the measurement noise covariance matrix.

Module 3 consists of two parts: the first part outputs the estimated GPS measurements, which is double the differenced measurements using the vehicle position estimated in Module 2 and the received ephemeris data of the observable satellites. The second part determines the integer ambiguity using the Wald test with the results of the first part and the GPS carrier measurements.

At the fixed known reference point A, the GPS measurement equation using the GPS carrier phase measurement is explained as follows. In general, errors in GPS carrier phase measurements include common and non-common errors. Common errors are those which have almost identical measurements between two or more nearby receivers: atmospheric error, satellite clock error, and satellites ephemeris error. Other errors are called non-common errors and include multipath errors and receiver errors [12].

$$\lambda\phi_A^i = \rho_A^i + \lambda N_A^i + e_{comman} + \varepsilon_A, \quad (13)$$

where ϕ_A^i is the carrier measurement, ρ_A^i is the true range, N is the integer ambiguity, e_{common} is the common error, and ε_A is the non-common error.

The linearized equation of 'A' with respect to an arbitrary point A_0 is derived as in (14):

$$\lambda\phi_A^i - \rho_{A0}^i = \begin{bmatrix} -\frac{x^i - x_A}{\rho_{A0}^i} & -\frac{y^i - y_A}{\rho_{A0}^i} & -\frac{z^i - z_A}{\rho_{A0}^i} \end{bmatrix} \cdot dX_A + \lambda N_A^i + e_{common} + \varepsilon_A$$
$$\rho_{A0}^i = \sqrt{(x^i - x_{A0})^2 + (y^i - y_{A0})^2 + (z^i - z_{A0})^2}, \quad (14)$$

where dX_A is a position vector between point A and point $A0$. Assuming that position 'A' is perfectly known, dX_A is 0. Then, the following equation (15) is obtained from (14):

$$\lambda\phi_A^i - \rho_A^i = \lambda N_A^i + e_{common} + \varepsilon_A. \quad (15)$$

In the same way, the linearized equation of 'B' with

$$\mathbf{F}_{11} = \begin{bmatrix} 0 & -\frac{v_E\tan L}{R_e+h} & \frac{v_N}{R_e+h} & 1 & 0 & 0 & 0 & 0 & 0 \\ \frac{v_E\tan L}{R_e+h} & 0 & \frac{v_E}{R_e+h} & 0 & 1 & 0 & 0 & 0 & 0 \\ -\frac{v_N}{R_e+h} & -\frac{v_E}{R_e+h} & 0 & 0 & 0 & 1 & 0 & 0 & 0 \\ \frac{g_n}{R_e+h} & 0 & 0 & 0 & -2\Omega\sin L - \frac{v_E\tan L}{R_e+h} & \frac{v_N}{R_e+h} & 0 & -f_D & f_E \\ 0 & \frac{g_n}{R_e+h} & 0 & 2\Omega\sin L + \frac{v_E\tan L}{R_e+h} & 0 & 2\Omega\cos L + \frac{v_E}{R_e+h} & f_D & 0 & -f_N \\ 0 & 0 & \frac{2g_n}{R_e+h} & -\frac{v_N}{R_e+h} & -2\Omega\cos L - \frac{v_E}{R_e+h} & 0 & -f_E & f_N & 0 \\ 0 & 0 & 0 & 0 & 0 & 0 & 0 & -\Omega\sin L - \frac{v_E\tan L}{R_e+h} & \frac{v_N}{R_e+h} \\ 0 & 0 & 0 & 0 & 0 & 0 & \Omega\sin L + \frac{v_E\tan L}{R_e+h} & 0 & \Omega\cos L + \frac{v_E}{R_e+h} \\ 0 & 0 & 0 & 0 & 0 & 0 & -\frac{v_N}{R_e+h} & -\Omega\cos L - \frac{v_E}{R_e+h} & 0 \end{bmatrix}, \quad \mathbf{F}_{12} = \begin{bmatrix} 0_{3\times 3} & 0_{3\times 3} \\ \mathbf{C}_b^n & 0_{3\times 3} \\ 0_{3\times 3} & -\mathbf{C}_b^n \end{bmatrix}$$

respect to an arbitrary point B_0 is derived as in (16):

$$\lambda\phi_B^i - \rho_{B0}^i = \left[-\frac{x^i - x_B}{\rho_{B0}^i} - \frac{y^i - y_B}{\rho_{B0}^i} - \frac{z^i - z_B}{\rho_{B0}^i}\right] \cdot dX_B, + \lambda N_B^i + e_{common} + \varepsilon_B$$
$$\rho_{B0}^i = \sqrt{(x^i - x_{B0})^2 + (y^i - y_{B0})^2 + (z^i - z_{B0})^2}, \quad (16)$$

where dX_B is a position vector between point B and point B_0.

For satellites i and j, (17) is the double differenced measurement equation between two receiver points 'A' and 'B'. After the differencing process, only non-common errors remain, as follows:

$$\lambda\nabla\Delta\phi_{AB}^{ij} - \nabla\Delta\rho_{AB0}^{ij} = h_{AB}^{ij} \cdot dX_B + \lambda\nabla\Delta N_{AB}^{ij} + \nabla\Delta\varepsilon_{AB},$$
$$\nabla\Delta\rho_{AB0}^{ij} = \left(\rho_{B0}^j - \rho_A^j\right) - \left(\rho_{B0}^i - \rho_A^i\right),$$
$$\nabla\Delta N_{AB}^{ij} = \left(N_B^j - N_A^j\right) - \left(N_B^i - N_A^i\right),$$
$$h_{AB}^{ij} = \left[-\frac{x^i - x_B}{\rho_{B0}^i} + \frac{x^j - x_B}{\rho_{B0}^j} \quad -\frac{y^i - y_B}{\rho_{B0}^i} + \frac{y^j - y_B}{\rho_{B0}^j} \quad -\frac{z^i - z_B}{\rho_{B0}^i} + \frac{z^j - z_B}{\rho_{B0}^j}\right]. \quad (17)$$

Also, (17) can be generalized to (18) with more satellites:

$$l = h \cdot dX_B + \lambda \cdot N + v,$$
$$l = \begin{bmatrix} \lambda\nabla\Delta\phi_{AB}^{ij} - \nabla\Delta\rho_{AB0}^{ij} \\ \lambda\nabla\Delta\phi_{AB}^{jk} - \nabla\Delta\rho_{AB0}^{jk} \\ \vdots \end{bmatrix}, \quad (18)$$
$$h = \begin{bmatrix} h_{AB0}^{ij} \\ h_{AB0}^{jk} \\ \vdots \end{bmatrix}, \quad N = \begin{bmatrix} \nabla\Delta N_{AB}^{ij} \\ \nabla\Delta N_{AB}^{jk} \\ \vdots \end{bmatrix},$$

where l is a double differenced residual vector, h is a double differenced observation matrix, N is a double differenced integer ambiguity, and v is a double differenced non-common error.

According to (19), the estimated carrier measurements are computed in Module 3. It is possible that the estimated GPS carrier measurement is obtained using the position of the satellites and the result of Module 2, which estimates the position of the mobile user using the integration algorithm. Finally, the new double differenced estimated measurement equation can be constructed as in (19):

$$\hat{l} = h \cdot d\hat{X}_B + \lambda \cdot \hat{N}, \quad (19)$$

where $d\hat{X}_B$ is the estimated state and $\hat{N}$ is the estimated integer ambiguity.

Through the difference between (18) and (19), the residual vector can be represented as in (20):

$$r_{GPS}(t) = (l - h \cdot d\hat{X}_B - \lambda \cdot \hat{N}),$$
$$r(t) = \begin{bmatrix} r_{GPS}(t) \\ r_{GPS/INS}(t) \end{bmatrix}, \quad (20)$$

where $r_\phi(t)$ is the GPS residual vector and $r(t)$ is the residual vector of the integrated GPS/INS. The Wald test is conducted using (21) and applying the residuals from (20).

$$F_i(k) = \frac{F_i(k-1) \cdot f_i\left(r(k)\right)}{\sum_{j=1}^{m} F_j(k-1) \cdot f_j\left(r(k)\right)}, \quad (21)$$

where $f_i(r(k)) = C \cdot \exp^{-\frac{1}{2} r_i(k)^T w_r r_i(k)}$, $Q_r = \begin{bmatrix} Q_{carrier} & 0 \\ 0 & Q_{GPS/INS} \end{bmatrix}$, and $W_r = Q_r^{-1}$.

4. EXPERIMENTAL RESULTS

To verify the performance of the proposed algorithm, an experiment was performed in Seoul, Korea. Fig. 3 shows the INS and GPS receivers used in the car for the experiment. The data was collected using the Black Diamond System (BDS), which includes an OEM4 GPS receiver, a Novatel GPS-600 antenna, and a Honeywell HG-1700 INS. Table 1

Table 1. Specifications of the INS and GPS receiver.

OEM4 (Novatel)	HG-1700 (Honeywell)
Position Accuracy: 1.8m CEP(Single Point L1),0.45m CEP(DGPS)	Gyro Input Range: ±1,000deg/sec
Velocity Accuracy: 0.03m/s RMS	Accelerometer Range: ±50 g
Time Accuracy: 20ns RMS	Output Data Rate: 100Hz
Data Rate: 20Hz	Gyro Bias: 10deg/hr
Measurement Precision: 6cm RMS(L1 C/A Code), 0.75mm RMS (L1 Carrier Phase)	Accelerometer Bias: 1.0 mg

shows the specifications of the INS and GPS receiver.

As seen in Fig. 3, one GPS antenna was installed on the roof rack of the car and the INS was installed inside the car. Fig. 4 shows the GPS receiver and the antenna of the reference station. An identical GPS system was used for the mobile user.

The experiment began with an initial static alignment of the INS for approximately 460 seconds, and then it was moved along a preplanned trajectory twice, as shown in Fig. 5. It took approximately 3 minutes to move around the planned trajectory once.

Fig. 3. GPS and INS for the mobile user.

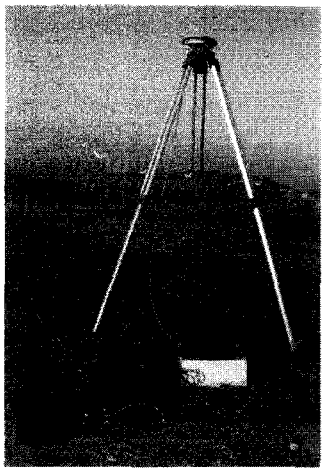

Fig. 4. GPS unit of the mobile reference station.

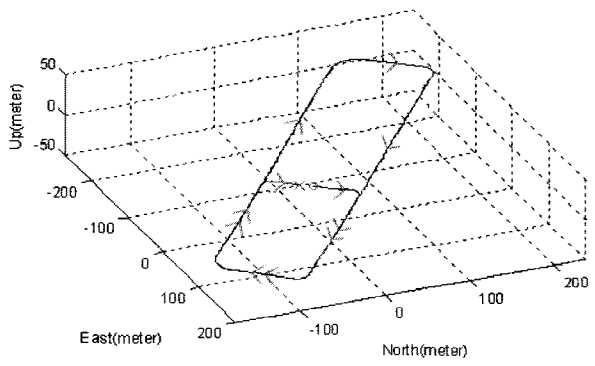

Fig. 5. Trajectory of the car during the experiment.

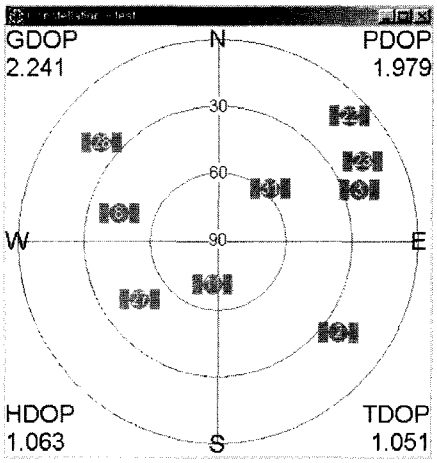

Fig. 6. Satellite constellation of the observable satellites.

Fig. 5 shows the trajectory of the car during the experiment.

Fig. 6 shows the satellite constellation of the observable GPS satellites at the beginning of the experiment. The nine visible GPS satellites appeared at the reference station, while only seven satellites were available in the mobile station during the experiment. The observable environment around the mobile station was not good because there were too many buildings and trees in the urban area. All data processing was performed by post-processing, but this algorithm can be implemented in a real time environment.

To analyze the performance of the proposed Wald test algorithm in resolving integer ambiguity with respect to the number of measurements or dilution of precision (DOP), the number of observable satellites was changed from seven to six, and finally to five. Figs. 7 and 8 show the position DOP (PDOP) and vertical DOP (VDOP) with respect to the number of observable satellites.

The results of the Wald test using seven observable satellites with and without the assistance of INS are

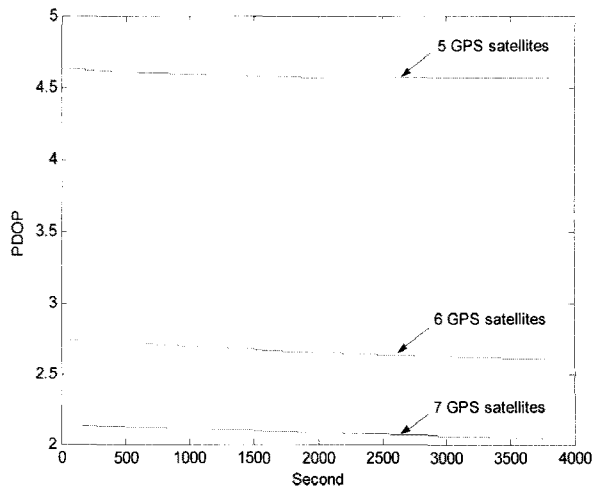

Fig. 7. PDOP.

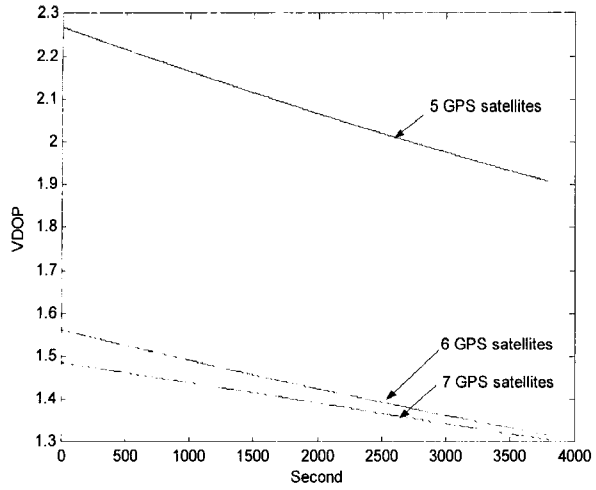

Fig. 8. VDOP.

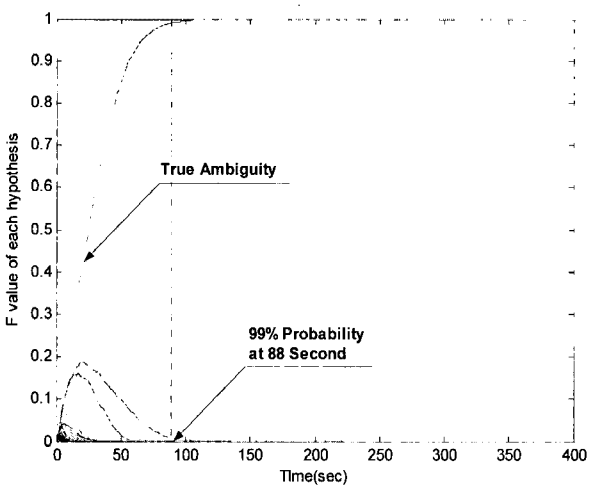

Fig. 9. Probability of the hypotheses using only seven GPS satellites.

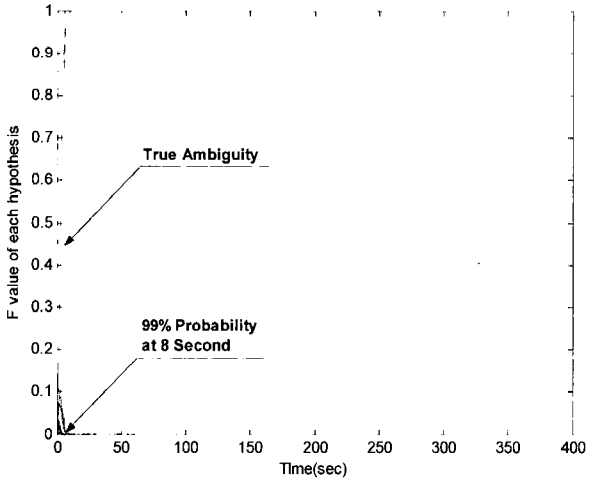

Fig. 10. Probability of the hypotheses using seven GPS satellites and INS.

shown in Figs. 9 and 10. Although the same probabilities are assigned to all integer candidates at the beginning, the results will have different probabilities as the Wald test sequentially processes the residuals. As the algorithm propagates, one integer

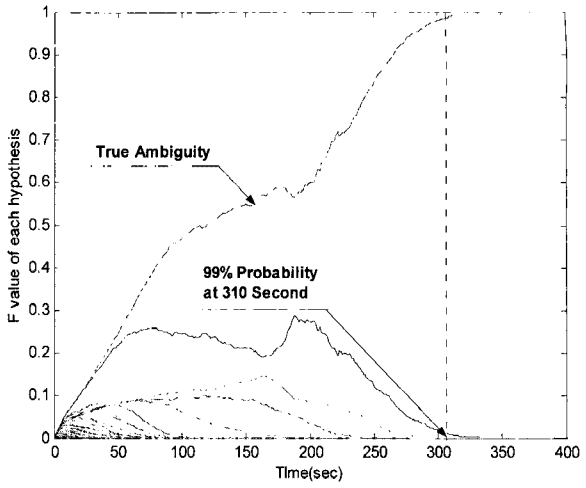

Fig. 11. Probability of the hypotheses using only six GPS satellites.

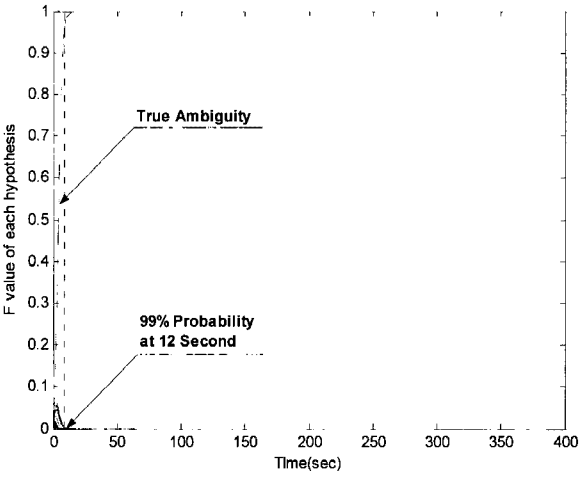

Fig. 12. Probability of the hypotheses using six GPS satellites and INS.

ambiguity, which is likely be true, will have a higher probability, leaving the remaining candidates with lower probabilities.

After beginning the experiment, the algorithm found the correct integer ambiguity after 88 seconds. Fig. 10 shows the probabilities of the hypotheses, which were predicted by the proposed algorithm using GPS and INS measurements. The integer ambiguity was found in 8 seconds.

Analyses were also performed by changing the number of visible satellites. For six GPS satellites, Fig. 11 shows that the integer ambiguity was determined after 310 seconds when using only the GPS. However, when using the GPS and INS measurements together, the integer ambiguity was determined after only 12 seconds. Comparing Figs. 10 and 12, there was only a small delay in obtaining convergence.

When the number of GPS satellite measurements was reduced from seven to six, it took approximately 200 seconds longer for the GPS only case. This means that the ambiguity resolution is very sensitive to the number of visible satellites. However, when using the

INS information as well as the GPS information, it took only 4 seconds longer than using seven satellites to obtain convergence, as seen by comparing Figs. 10 and 12. Therefore, the proposed algorithm obtains a faster convergence and is less sensitive to the number of observable satellites.

Finally, the number of visible satellites was reduced from six to five. Fig. 13 shows the probabilities of the hypotheses using only the GPS measurements. The Wald test fails to find the true integer ambiguity: the small number of GPS satellites makes this difficult. However, Fig. 14 shows how the lack of sufficient GPS satellites is overcome with the help of the INS measurements. It took 15 seconds to obtain the true integer ambiguity. The INS information for the proposed algorithm helps obtain one true integer from many candidates. This shows that the INS measurements provide the high quality information needed to accelerate the process of attributing a high probability to the true candidate and low probabilities to all others. Finally, this process results in a faster convergence time in resolving the integer.

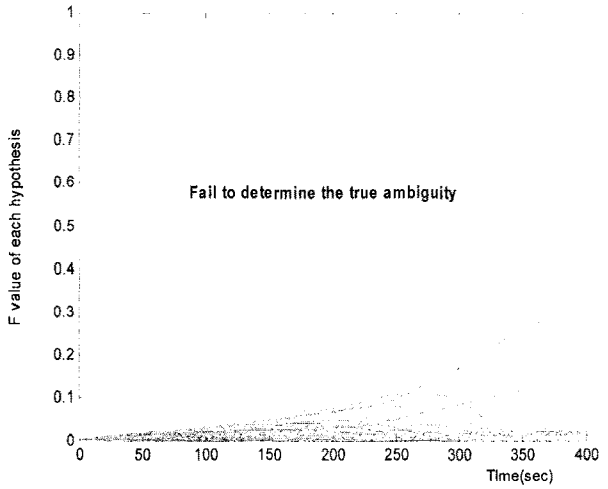

Fig. 13. Probability of the hypotheses using only five GPS satellites.

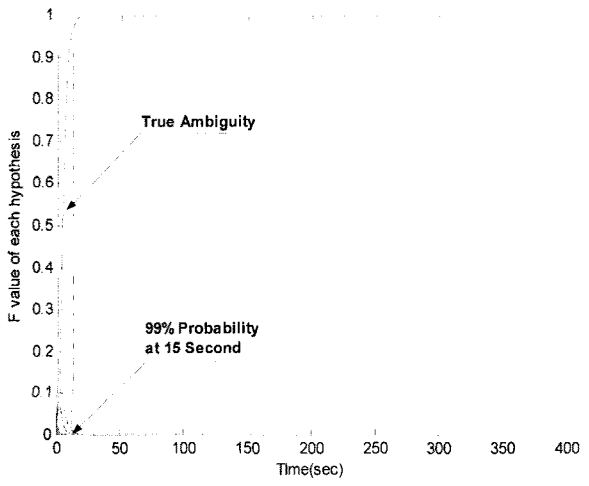

Fig. 14. Probability of the hypotheses using only five GPS satellites and INS.

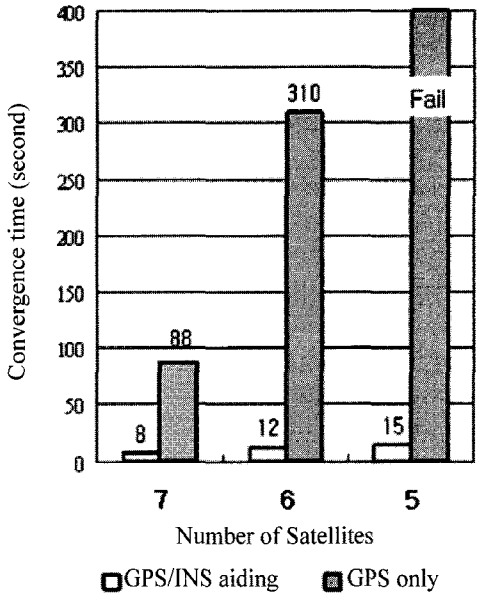

Fig. 15. Summary of the convergence times.

Furthermore, it works as one measurement and eventually succeeds in obtaining the integers using only five observable satellites, where the normal algorithm fails to obtain them.

Fig. 15 summarizes the convergence time of the experiment performed.

Summarizing the experimental results, it is clear that the impact of the INS information on the Wald test in resolving integer ambiguity is positive. Furthermore, for smaller numbers of observable satellites, the performance improvement in the convergence time is very significant when the INS information is used. In the case of five visible satellites, the GPS-only ambiguity resolution failed, but the integer ambiguity was resolved rapidly when using the added INS measurements.

5. CONCLUSIONS

Real time applications of GPS carrier phase measurements have been used for precise navigation for more than a decade. The primary problem in using carrier phase measurements as high accuracy range measurements for real time navigation is resolving the integer ambiguity in real time and in real situations.

In this paper, a reduction in the convergence time in determining the integer ambiguity has been achieved using the Wald test together with INS information. Furthermore, this method enables the determination of integers even when as few as five satellites are observable.

To evaluate the proposed algorithm, an experiment was conducted. One GPS antenna was installed on a roof rack of a car and an INS was installed inside the car which moved along a preplanned trajectory twice with seven observable satellites. It was determined that it took 88 seconds to obtain convergence on the

integer ambiguity using the Wald test without the INS information; however, it took only 8 seconds for the proposed algorithm using the INS information. The positive impact of the INS information on the convergence time in the Wald test became greater when the number of observable satellites was reduced. For six observable GPS satellites, the integer ambiguity was determined in 310 seconds for the GPS-only case, whereas it took only 12 seconds when using the GPS and INS information together. With a fewer number of observable satellites, the ambiguity resolution occurred faster using the proposed algorithm with the INS information. Furthermore, when the number of visual satellites was five, the integer ambiguity could not be obtained; however, when the INS measurements were used, the integer ambiguity was successfully resolved within a reasonable time.

The experimental results have shown that the proposed Wald test algorithm used together with the INS information gives a much less sensitive convergence performance. Furthermore, the proposed method works as an additional measurement and eventually succeeds in obtaining integers with only five observable satellites where the normal algorithms fail to obtain them.

REFERENCES

[1] P. J. G. Teunissen, "The least-squares ambiguity decorrelation adjustment: A method for fast GPS integer ambiguity estimation," *Journal of Geodesy*, vol. 70, no. 1-2, pp. 65-82, November 1995.

[2] J. D. Wolfe, W. R. Williamson, and J. L. Speyer, "Hypothesis testing for resolving integer ambiguity in GPS," *Navigation: Journal of the Institution of Navigation*, vol. 50, no. 1, pp. 45-56, March 2003.

[3] M. F. Abdel-Hafez, Y. J. Lee, W. R. Williamson, J. D. Wolfe, and J. L. Speyer "A high-integrity and efficient GPS integer ambiguity resolution method," *Navigation: Journal of the Institute of Navigation*, vol. 50, no. 4, pp. 295-310, November 2003.

[4] D. H. Titterton and J. L. Weston, *Strapdown Inertial Navigation Technology*, Stevenage, U. K., Peregrinus, 1997.

[5] M. Forrest, T. Spracklen, and N. Ryan, "An inertial navigation data fusion system employing an artificial neural network as the data integrator," *Proc. ION NTM*, Anaheim, CA, pp. 153-158, January 2000.

[6] N. El-Sheimy and K. P. Schwarz, "Integrating differential GPS receivers with an inertial navigation system (INS) and CCD cameras for a mobile GIS data collection system," *Proc. of ISPRS94*, Ottawa, Canada, pp. 241-248, October 1994.

[7] S. Hong, Y. Chang, S. Ha, and M. Lee, "Estimation of alignment error in GPS/INS integration," *Proc. of ION GPS 2002*, Portland, Oregon, pp. 527-534, September 2002.

[8] M. G. Petovello, M. E. Cannon, G. Lachapelle, J. Wang, C. K. H. Wilson, O. S. Salychv, and V. V. Voronov, "Development and testing of a real-time GPS/INS reference system for autonomous automobile navigation," *Proc. of ION GPS 2001*, Salt Lake City, Utah, pp. 2634-2641, September 2001.

[9] K. Chiang and E. Naser, "GPS/INS integration using neural networks for land vehicle navigation applications," *Proc. of ION GPS 2002*, Portland, Oregon, pp. 535-544, September 2002.

[10] E. Lee, S. Chun, Y. J. Lee, T. Kang, G. Jee, and M. F. Abdel-Hafez, "Performance improvement of wald test for resolving GPS integer ambiguity using a baseline-length constraint," *International Journal of Control, Automation, and Systems*, vol. 4, no. 3, pp. 333-343, June 2006.

[11] J. Seo, H. K. Lee, J. G. Lee, and C. G. Park, "Lever arm compensation for GPS/INS/odometer integrated system," *International Journal of Control, Automation, and Systems*, vol. 4, no. 3, pp. 333-343, June 2006

[12] C. Park, D. J. Cho, E. J. Cha, D.-H. Hwang, and S. J. Lee, "Error analysis of 3-dimensional GPS attitude determination system," *International Journal of Control, Automation, and Systems*, vol. 4, no. 4, pp. 480-485, 2006.

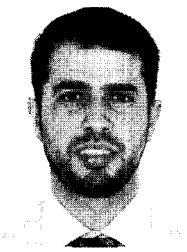

Mamoun F. Abdel-Hafez is an Assistant Professor in the Department of Mechanical Engineering at the American University of Sharjah, Sharjah, United Arab Emirates. He received the M.S. in Mechanical Engineering from the University of Wisconsin, Milwaukee in 1999, and the Ph.D. degree in Mechanical Engineering from the University of California, Los Angeles (UCLA) in 2003. His research interests are in stochastic estimation, control systems, and algorithms and applications of GPS/INS systems.

Dae Je Kim is a Research Engineer in R&D center at the Hyundai Rotem, Korea. He received the M.S. degree in Aerospace Engineering at the Konkuk University in 2004. His research interests are integrated navigation system, obstacle avoidance for unmanned ground vehicles.

Eunsung Lee is a Senior Researcher in the Satellite Navigation System Department at the Korea Aerospace Research Institute. He received the Ph.D. degree in Aerospace Engineering from Konkuk University in 2005. His research areas include GPS RTK, orbit determination, and fault detection of GPS systems.

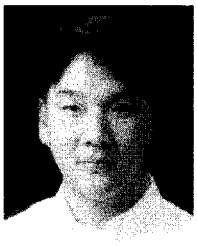

Sebum Chun is a Senior Research Engineer in Microinfinity Co., Ltd. He received his M.S. degree in Aerospace Engineering from the Konkuk University, Korea in 2002. He received the Ph.D. degree in Aerospace Engineering from Konkuk University in 2008. His research areas include GPS/INS/Vision system integration, GPS RTK and nonlinear estimation.

Young Jae Lee is a Professor in the Department of Aerospace Engineering at Konkuk University, Korea. He received the Ph.D. degree in Aerospace Engineering from the University of Texas at Austin in 1990. His research interests include integrity monitoring of GNSS signal, GBAS, RTK, attitude determination, orbit determination, and GNSS related engineering problems.

Teasam Kang is an Associate Professor of the Department of Aerospace Engineering at Konkuk University, Korea. He received the B.S., M.S., and Ph.D. degrees from the Seoul National University in 1986, 1988 and 1992, respectively. His current research areas are robust control theories and its applications that include flight control, development of micro aerial vehicle, and MEMS inertial sensor development.

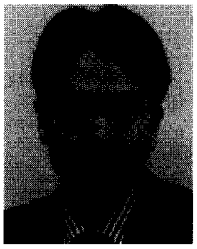

Sangkyung Sung received the B.S., M.S., and Ph.D. degrees in School of Electrical Engineering from Seoul National University, Seoul, Korea, in 1996, 1998, and 2003, respectively. From March 1996 to February 2003, he worked for Automatic Control Research Center in Seoul National University. Currently, he is an Assistant Professor of department of aerospace information engineering, Konkuk University, Seoul, Korea. His research interests are avionics sensor, nonlinear and robust control, micro inertial sensor and estimation and filtering theory.